Magnetism in polymorphic phases: Case of $PrIr_2Si_2$

M. Mihalik,* M. Diviš, and V. Sechovský
Faculty of Mathematics and Physics, Department of Condensed Matter Physics, Charles University, Ke Karlovu 5, 121 16 Prague 2, Czech Republic

N. Kozlova and J. Freudenberger
IFW Dresden, Helmholtzstraße 20, 01069 Dresden, Germany

N. Stüßer and A. Hoser
Helmholtz-Centre Berlin for Materials and Energy, Hahn-Meitner-Platz 1, 14109 Berlin, Germany
(Received 14 December 2009; revised manuscript received 19 April 2010; published 28 May 2010)

We have pursued a comparative study of magnetism in the two polymorphic phases of $PrIr_2Si_2$ in order to demonstrate how magnetism is influenced by changing the crystallographic symmetry while the chemical composition remains conserved. For this purpose we have prepared single crystals of the α and β phase of $PrIr_2Si_2$, and measured magnetization, ac susceptibility, specific heat, and electrical resistivity as functions of temperature and magnetic field and performed neutron-diffraction experiments in magnetic field. We have confirmed that the β phase remains paramagnetic down to 2 K whereas the α phase exhibits ordering of the Pr magnetic moments at temperatures lower than T_N=45.5 K. We have found two different magnetic structures: the first a longitudinal sine-modulated structure with a magnetic propagation vector $\boldsymbol{k}=(0\ 0\ 5/6)$ at temperatures $23.7<T<45.5$ K and the second a simple antiferromagnetic structure with $\boldsymbol{k}=(0\ 0\ 1)$ for $T<23.7$ K. The phases can be destabilized by applying a magnetic field along the c axis while they remain intact if the magnetic field is applied along the a axis. In both magnetic phases, the Pr^{3+} ion has a stable magnetic moment of $3.2\mu_B$. Another striking difference in magnetism between the α and β phase of $PrIr_2Si_2$ is observed in the type of magnetocrystalline anisotropy, easy axis (easy plane) in the α phase (β phase). The different anisotropy types for the α and β phase are corroborated by results obtained from first-principles crystal-field calculations based on density-functional theory.

DOI: 10.1103/PhysRevB.81.174431 PACS number(s): 75.50.Ee, 75.30.−m, 61.05.fm, 61.50.Ah

I. INTRODUCTION

In 1983, Braun *et al.*[1] discovered the compound $LaIr_2Si_2$ and observed that it adopts two different crystallographic structures depending on thermal history. The as-cast sample, containing the β phase is stable at high temperatures and remains in the rapidly cooled as-cast sample at room temperature and lower as a metastable phase exhibiting the $CaBe_2Ge_2$-type structure (space group $P4/nmm$). The slow cooled sample (α phase) shows the $ThCr_2Si_2$-type structure (space group $I4/mmm$),[1] which is the true stable phase at room temperature and below. Both structures are tetragonal but are formed by different stacking of the Th(Ca), Cr(Be), and Si(Ge) atomic basal planes along the c axis. In 1985, Hoffmann and Zheng[2] calculated the X-X bonding energy in the AB_2X_2-type compounds and found that there can be two energy minima caused by the "bonding," "Coulomb," and "packing" requirements. As a consequence of the two minima, they discussed possible polymorphism in this type of compounds.[2] Analogous polymorphism to the $LaIr_2Si_2$ case has been found in a number of other 122 compounds: $RENi_2As_2$ (RE=La, Ce, Pr, Nd, and Sm), UCo_2Ge_2, $CeIr_2Si_2$, and $YbIr_2Si_2$.[3–7]

The first paper published on $PrIr_2Si_2$ reported that the compound adopted only the $ThCr_2Si_2$-type crystal structure[8] contrary to the polymorphism confirmed in other $REIr_2Si_2$ compounds (RE=La,Ce,Nd,Yb).[1,6,7,9] This apparent controversy attracted our attention and recently we confirmed that $PrIr_2Si_2$ shows polymorphism where the α to β transition occurs above 300 °C (Ref. 10) and that the β phase is metastable at room temperatures as found in $LaIr_2Si_2$.[1]

The isolation of both of polymorphs of $REIr_2Si_2$ (RE=La,Ce,Pr,Nd) at low temperatures offers a unique possibility of comparative investigation of the impact the two different crystallographic symmetries on electronic structure and related physical properties of the same compound without changing chemical composition. It has already been demonstrated that α-$LaIr_2Si_2$ is a normal metal down to 1 K whereas β-$LaIr_2Si_2$ is superconducting at 1.6 K.[1] Both $CeIr_2Si_2$ phases exhibit no magnetic ordering: the α phase behaves as a normal Fermi liquid and the β phase exhibits non-Fermi-liquid attributes.[11] $PrIr_2Si_2$ is particularly interesting because the electron states of Pr^{3+}, as a non-Kramers ion, are very sensitive to the crystal-field (CF) symmetry.

The first paper on magnetism in $PrIr_2Si_2$, published by Welter *et al.*,[8] focused only on the α phase and reported antiferromagnetism below T_N=47 K with an order-to-order magnetic phase transition at T_t=25 K. The experiments were performed on polycrystalline samples and therefore offered no information about anisotropy in the compound. However, strong magnetocrystalline anisotropy has often been reported for RET_2X_2 (RE=rare-earth element, T=transition metal, and X=p-electron element) compounds.[12–14]

We succeeded in preparing single crystals of both α-$PrIr_2Si_2$ and β-$PrIr_2Si_2$. In the preliminary study, no indication of magnetic ordering has been observed in the β phase whereas antiferromagnetism with a complex magnetic phase

diagram has been indicated for α-$PrIr_2Si_2$.[15] In this paper we present and discuss results of a comprehensive set of experiments (studying the specific heat down to low temperatures in magnetic fields, ac susceptibility, electrical resistivity, and magnetoresistivity, magnetization in fields up to 40 T, and examine in more detail the magnetic structure using neutron diffraction, also in applied magnetic fields) to understand the different aspects of the physics of the two polymorphs of $PrIr_2Si_2$.

II. SAMPLE PREPARATION AND EXPERIMENTAL SETUP

The preparation details of the samples are reported in our previous article.[15] For measuring the bulk physical properties and the single-crystal neutron-diffraction experiments, we used the single-crystal samples from the same grown rod as in our previous article.[15] For the neutron powder-diffraction experiment polycrystalline samples were used, obtained by arc melting a stoichiometric mixture of the starting elements. The polycrystalline samples were annealed at 900 °C for 6 h in order to replicate the synthesis conditions of the single crystal. After this procedure the samples were checked by x-ray powder diffraction, confirming single phase α-$PrIr_2Si_2$. To facilitate the analysis of the specific-heat data for the two $PrIr_2Si_2$ phases, $LaIr_2Si_2$ in polycrystalline form was also measured as a nonmagnetic analog. An analogous preparation procedure was used for the $LaIr_2Si_2$ samples.

The powder neutron-diffraction experiment was performed on the E6 diffractometer at the Helmholtz-Zentrum Berlin using a standard Orange cryostat, and a two position-sensitive two-dimensional (2D) detectors.[16] A neutron wavelength of 2.44 Å was used. Full pattern data ($6° < 2\theta < 108°$) were collected at 1.5, 30, 50, and 300 K as well as a series of narrow patterns ($33° < 2\theta < 48°$) at temperatures around T_t. Since iridium is quite a strong neutron absorber, a 5-mm-diameter sample was used. The effect of absorption was taken into account when fitting experimental data using FULLPROF.[17]

The standard notation for the angles is used as defined for a four-circle neutron diffractometer for the single-crystal neutron experiment.[18] Only the α-$PrIr_2Si_2$ crystal was measured on E6 using the HM-1 horizontal field magnet. The scattering plane was defined by the (002) and (110) reciprocal vectors and we studied the $(-1-1\ 0+q)$ magnetic reflection. Our first goal was to apply the magnetic field along the c axis but the accessible Q space did not allow such an experiment. Instead, we rotated the sample in the magnet 4° out of the magnetic field direction and scanned through the magnetic reflection by rotating the sample inside the magnet. This resulted in a variation in the misalignment of the magnetic field with respect to the c axis in the range from −12° to +4°. Since α-$PrIr_2Si_2$ exhibits strong uniaxial anisotropy,[15] we believe that this misalignment induced no spurious effects on the magnetic state of this compound. Taking into account only the component of the magnetic field along the c axis, the real magnetic field varied between 5.89 and 6 T during the scan at the 6 T set point, and between 3.91 and 4 T at the 4 T set point.

The high magnetic field magnetization measurements were done at the pulsed field facility at IFW, Dresden using the 50 T pulse magnet.[19] We performed pulses up to 40 T at 4.2 K for the β-phase sample and at $4.2 < T < 50$ K for the accidentally mixed (spontaneously partially recrystallized) α- and β-phase samples. In magnetic fields higher than 20 T, no effects other than the weak linear increase were observed for both samples. Therefore we limited further measurements on longer pulses with the maximal field to 20 T at several temperatures in temperature range 4.2–40 K. Since data up to 20 T from the 20 T and 40 T pulse coincided, we can conclude that the eddy currents induced in the sample due to the fast magnetic field change do not significantly influence the result of the experiment. The resistivity and specific heat were measured using a Physical Property Measurement System (PPMS) (Quantum Design) apparatus whereas the ac susceptibility and dc magnetization measurements were done using the Magnetic Property Measurement System (MPMS) apparatus (also from Quantum Design).

III. RESULTS

A. $LaIr_2Si_2$

The temperature dependence of the specific heat of $LaIr_2Si_2$ was considered to be a sum of the electronic C_{el} ($=\gamma T$) and phonon (lattice) C_{ph} contribution, respectively. For the purposes of this paper it was sufficient to describe C_{ph} using only the Debye theory,[20]

$$C_{ph} = 9R\frac{1}{1-\alpha_D T}\left(\frac{T}{\theta_D}\right)^3 \int_0^{\theta_D/T} \frac{x^4 e^x}{e^x - 1} dx. \qquad (1)$$

In this equation R is the gas constant, θ_D is the Debye temperature, and α_D is the correction to the anharmonicity of the phonons. This equation can be approximated by a cubic dependency at low temperatures—the well known T^3 law.

The specific heat of the both phases is linear in the C/T vs T^2 plot in the temperature range 2–6.7 K for the α-$LaIr_2Si_2$ and in the region 5–6.7 K for the β-$LaIr_2Si_2$. The deviation from linearity below 5 K for the case of β-$LaIr_2Si_2$ is connected with the transition to the superconducting phase, which takes place at 1.6 K.[1] From fitting the T^3 law in the above-mentioned temperature ranges, we have derived the electronic contribution to the specific heat to be 8.78 mJ mol^{-1} K^{-2} for the α phase, and 3.54 mJ mol^{-1} K^{-2} for the β phase. As the next step C_{el} was fixed and only C_{ph} was fitted using Eq. (1) in the whole temperature range. The fit converged to the parameters $\theta_D = 265$ K, $\alpha_D = 1.3 \times 10^{-3}$ K^{-1} for the α-$LaIr_2Si_2$ and $\theta_D = 233$ K, $\alpha_D = 1.6 \times 10^{-3}$ K^{-1} for the β-$LaIr_2Si_2$. The difference between the values of the Debye temperature can be attributed to the different crystal symmetry. Using only C_{el} and C_{ph} terms for the description of the specific heat of $LaIr_2Si_2$ resulted in a satisfactory match between experimental data and theoretical results (Fig. 1). This allowed us to use $LaIr_2Si_2$ as a nonmagnetic analog of $PrIr_2Si_2$, which substantially simplified the analysis of the specific heat of both phases of $PrIr_2Si_2$.

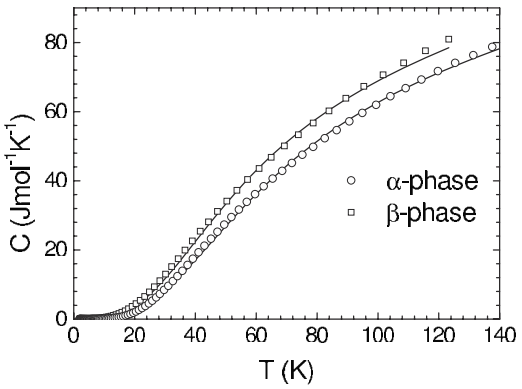

FIG. 1. The specific heat of $LaIr_2Si_2$. The lines represent the best fit due to electronic and phonon contribution as described in the text.

B. β-$PrIr_2Si_2$

Using the comparative analysis of specific heat with β-$LaIr_2Si_2$ as nonmagnetic analog, we calculated the magnetic contribution to C_{mag} in β-$PrIr_2Si_2$ (see Fig. 2). As expected for the rare-earth-based intermetallic compounds, we observed an anomaly in $C_{mag}(T)$, represented by the two bumps with maxima around 5 K and around 50 K. We attributed this anomaly to the Schottky contribution to C_{mag} that was fitted using[21]

$$C_{sch} = \frac{R}{T^2}\left\{\frac{\sum_{i=0}^{n}\Delta_i^2 \exp(-\Delta_i/T)}{\sum_{i=0}^{n}\exp(-\Delta_i/T)} - \left[\frac{\sum_{i=0}^{n}\Delta_i \exp(-\Delta_i/T)}{\sum_{i=0}^{n}\exp(-\Delta_i/T)}\right]^2\right\}, \quad (2)$$

where Δ_i is the position of the ith crystal-field level expressed in kelvin.

We were able to determine five Schottky levels: 0 K (fixed level), 8.8(6) K, 23(2) K, 140(10) K, and 170(20) K. We note that the tetragonal crystal field at the Pr site splits the ground state of the Pr^{3+} ion into nine singlet states. The remaining four singlet states are probably located at much higher energy and we could not determine them. Such a large Schottky splitting already points to the strong crystal field in this compound. The fact that there are only five populated levels at temperatures lower than 80 K is also evident from the magnetic entropy (Fig. 2). As one expects for the five-level system, the magnetic entropy approaches the value $R \ln 5$ (=13.38 J mol^{-1} K^{-1}) at 80 K.

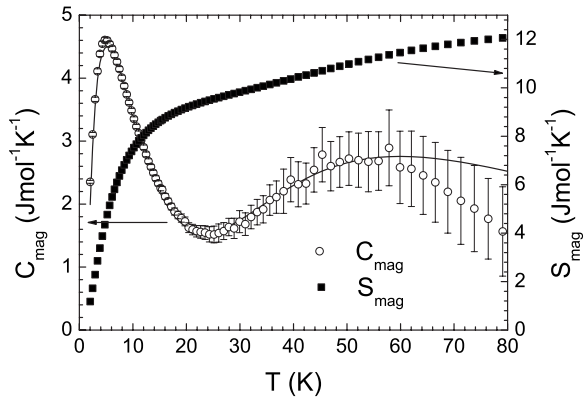

FIG. 2. The magnetic part of the specific heat of β-$PrIr_2Si_2$ plotted together with the calculated corresponding magnetic entropy. The solid line in the figure represents the best fit due to the Schottky contribution.

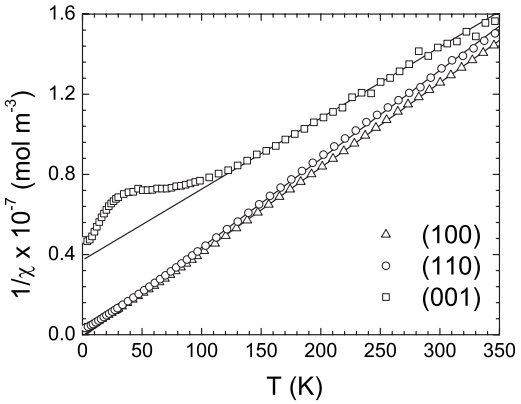

FIG. 3. The inverse susceptibility of the β phase. The lines represent the best fit with the Curie-Weiss law.

In order to investigate the magnetocrystalline anisotropy dc susceptibility in a magnetic field applied along the (100), (110), and (001) crystallographic directions was measured. The temperature dependences of the inverse dc susceptibility $(1/\chi)$ (Fig. 3) measured with the magnetic field applied along the (100) (a axis) and the (110) (basal-plane diagonal) compare well, whereas data obtained for the (001) (c-axis) direction differ considerably. Therefore, one can conclude that the susceptibility exhibits negligible anisotropy within the basal plane and a considerable anisotropy between the c axis and the basal plane.

The $1/\chi$ vs T dependences displayed in Fig. 3 are linear over a limited high-temperature intervals which can be fitted to the Curie-Weiss law,[22]

$$\chi = \frac{C}{T - \theta_p} \quad (3)$$

in the corresponding temperature ranges. In Eq. (3) the Curie constant $C = N\mu_{eff}^2$, where N=Avogadro number, n =number of ions (in the formula unit) carrying the magnetic moment and μ_{eff}=effective magnetic moment. The fitting parameters and the temperature intervals of fitted data are summarized in Table I. The fitted values of the effective moment are somewhat higher than the effective moment calculated for a free Pr^{3+} ion ($3.58\mu_B$). Existence of an effective magnetic moment of $0.88-1.59\mu_B$ on Ir would serve as one of a possible explanations of the enhanced values of the fitted effective moment. A more plausible scenario, however, involves the crystal-field effect which can divert the temperature dependence of the susceptibility from the unperturbed Pr^{3+} paramagnetic response at high temperatures toward a lower slope of the $1/\chi$ vs T dependence in the (lower) temperature region of our experiment.

TABLE I. The comparison of the fitted parameters according to the Curie-Weiss law.

	β phase			α phase		
Crystallographic direction	Fit range (K)	θ_p (K)	μ_{eff} (μ_B)	Fit range (K)	θ_p (K)	μ_{eff} (μ_B)
(100)	50–350	2.88	3.88	150–300	−228	4.23
(110)	50–350	1.43	3.79	200–320	−194	4.02
(001)	150–350	−105	4.23	200–300	52.5	4.02

The presence of the strong crystal field in this compound is obvious from our high-field magnetization data. In Fig. 4 it is seen that the a-axis magnetic moment reaches 2.3 μ_B/f.u. at T=4.2 K and B=40 T (the highest field of our measurements) and tends to saturate while the c-axis magnetization is approximately linear up to 40 T with no tendency to saturation. Extrapolating the c-axis magnetization to higher fields gives 2.3 μ_B/f.u at B=180 T, which may be taken as a very rough estimation of the magnetocrystalline anisotropy field in β-$PrIr_2Si_2$.

To describe the measured magnetization curves we used the framework of the mean-field approximation. According to this approximation, each Pr^{3+} ion feels an internal field,

$$H = B + \lambda M, \tag{4}$$

where B is the external magnetic field, M is the magnetization, and λ is the mean-field constant. The magnetization should obey the equation[22]

$$M = M_{sat} B_J(x), \tag{5}$$

where M_{sat} is the saturated magnetization and $B_J(X)$ is the Brillouin function given by

$$B_J(x) = \frac{2J+1}{2J}\coth\frac{2J+1}{2J}x - \frac{1}{2J}\coth\frac{1}{2J}x. \tag{6}$$

In the Brillouin function J (=4) is the total angular momentum and $x = g(JLS)\mu_B J(B+\lambda M)/(kBT)$, where $g(JLS)$ (=0.8) is the Landé g factor, μ_B is the Bohr magneton, k_B is the Boltzmann constant, and T (=4.2 K) is the temperature of the system. The problem with Eq. (5) is that the magnetization appears on the left side but, due to mean-field approximation also inside the Brillouin function [Eq. (6)]. This problem was overcome by introducing directly the measured magnetization data into the Brillouin function. Using this description we fitted only λ and M_{sat}. When approximating the a-axis data by a Brillouin function one obtains the mean-field constant −0.8 T/μ_B and a saturated magnetic moment of 2.3 μ_B/f.u. The latter value is considerably smaller than the theoretical ordered magnetic moment calculated for a free Pr^{3+} ion (3.20μ_B). A possible explanation for this discrepancy is that a small magnetic moment (~0.4μ_B/Ir) is induced (oriented antiparallel to the Pr moments) on the Ir site. A more plausible scenario considers a reduced Pr moment due to the crystal field influence on the Pr^{3+} ion. The c-axis moment exhibits a weak and linear increase with the field yielding a value of only 0.5 μ_B/f.u. in 40 T. This observed strong anisotropy corroborates the crystal-field scenario. The low-temperature magnetization curves and temperature dependences of the dc susceptibility for different crystallographic directions can be interpreted in terms of the easy (basal) plane anisotropy in β-$PrIr_2Si_2$.

The resistivity measured along the main crystallographic axes exhibits a metallic behavior at temperatures higher than 50 K. The residual resistivity ratio reaches only 2.3 for the c axis and 1.8 for the a axis.

At lower temperatures, the resistivity passes through a broad feature which has maximum around 20 K (Fig. 5). This feature can be suppressed by applying the field along the a axis but remains if the field is applied along the c axis. The latter result also corroborates the scenario of easy-plane

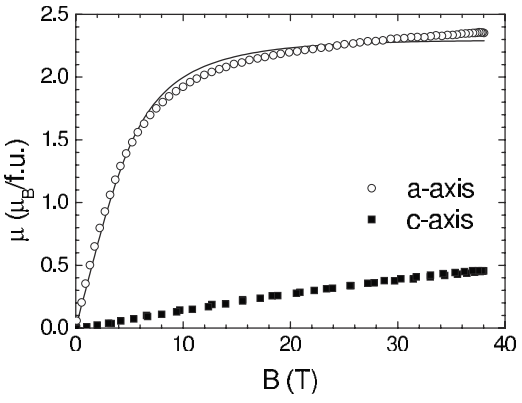

FIG. 4. The magnetization curves of the β phase measured up to 40 T at T=4.2 K. The line represents the best fit according to Eq. (5) in the main text.

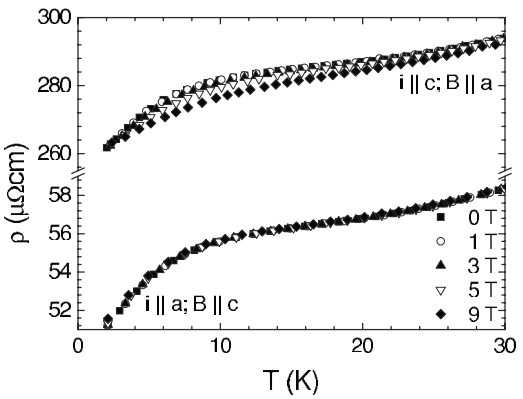

FIG. 5. The low-temperature detail of the resistivity of β-$PrIr_2Si_2$.

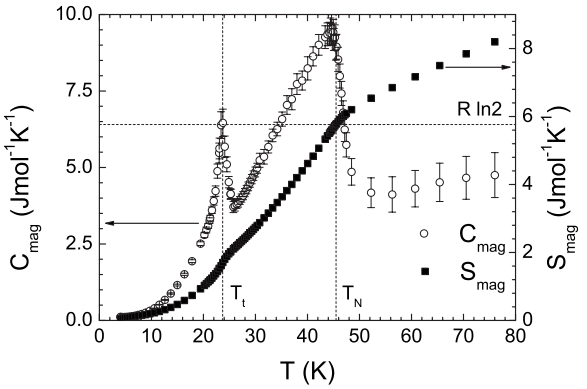

FIG. 6. The magnetic part of the specific heat of α-$PrIr_2Si_2$ plotted together with the calculated corresponding magnetic entropy.

anisotropy in β-$PrIr_2Si_2$. A similar feature in the low-temperature resistivity was observed for PrRhSn (Ref. 23) and we tentatively attribute this effect to the crystal-field influence.

C. α-$PrIr_2Si_2$

The magnetic specific heat of the α phase (Fig. 6) exhibits two well-distinguished peaks at T_N=45.5 K and T_t=23.7 K, respectively. The T_N and T_t values are in very good agreement with the transition temperatures presented by Welter *et al.*[8] In addition, we observe some contribution due to the splitting of the ground-state multiplet. Unfortunately, Schottky theory of the crystal-field splitting is not applicable to data in the ordered state (below T_N) and at temperatures higher than T_N the error bars are too high to obtain reliable information.

To calculate the magnetic entropy of α-$PrIr_2Si_2$ (Fig. 6) only the magnetic specific-heat data for temperatures higher than 4 K and corresponding data for the nonmagnetic analog α-$LaIr_2Si_2$ were taken into account. Below 4 K there is a significant contribution to the total specific heat due to the nuclear term (C_N) and therefore we have *ad hoc* interpolated the magnetic entropy in this region by linear interpolation to

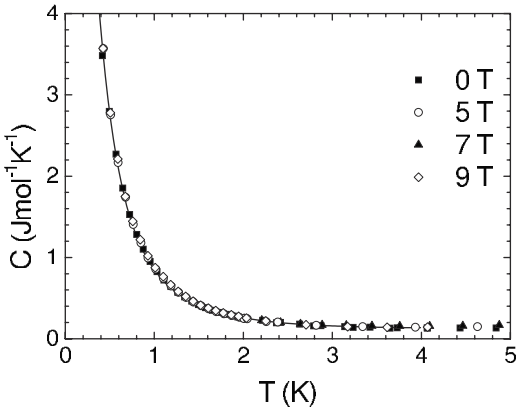

FIG. 7. The low-temperature detail of the α-phase specific heat shows the upturn caused by the nuclear contribution to the specific heat. The line represents the best fit using the Eq. (7).

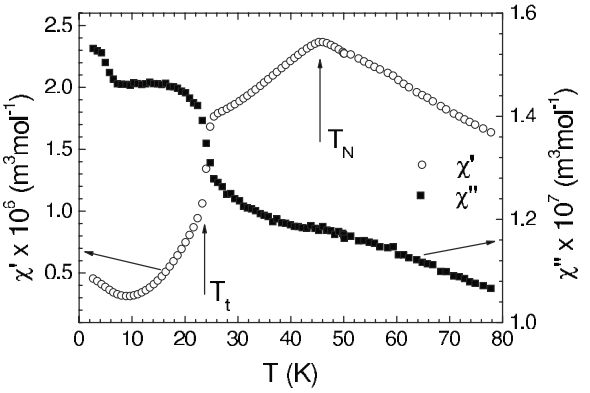

FIG. 8. ac susceptibility of α-$PrIr_2Si_2$ measured with driving frequency of 1000 Hz with a driving field amplitude of 0.001 T applied along the c axis. The upturn of the data for temperatures below 5 K is probably the impurity effect.

the point S=0 J mol^{-1} K^{-1} at T=0 K. At T_N the magnetic entropy only exhibits a change in slope, indicating that this phase transition is second order. Also, the magnetic entropy reaches only R ln 2 at T_N, which is theoretically the lowest expected limit for the magnetic ordering phase transition. At T_t, where the order-order transition occurs, the magnetic entropy is only 1.7 J mol^{-1} K^{-1}.

Below 4 K we found a large increase in the specific heat (Fig. 7) that is independent of the magnetic field up to 9 T. We assumed that this upturn is caused by the hyperfine field acting on the nuclei of the Pr^{3+} ions and we have fitted it according to[24]

$$C_N = -R\left(\frac{x^2}{4}\right)\left\{(2I+1)^2\mathrm{csch}^2\left[(2I+1)\frac{x}{2}\right] - \mathrm{csch}^2\left[\frac{x}{2}\right]\right\}, \tag{7}$$

where R is the gas constant, I is the nuclear angular momentum, and $x=\mu_N H/Ik_BT$, where μ_N is the nuclear magneton, k_B is the Boltzmann constant, and H is the hyperfine magnetic field. The determined hyperfine magnetic field is 316(5) T, which is very close to the hyperfine field in the pure Pr metal [326(1) T] and to the hyperfine field of

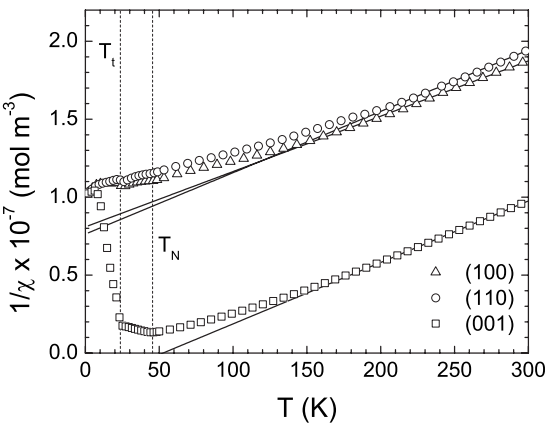

FIG. 9. The inverse susceptibility of the α phase. The lines represent the best fit with the Curie-Weiss law.

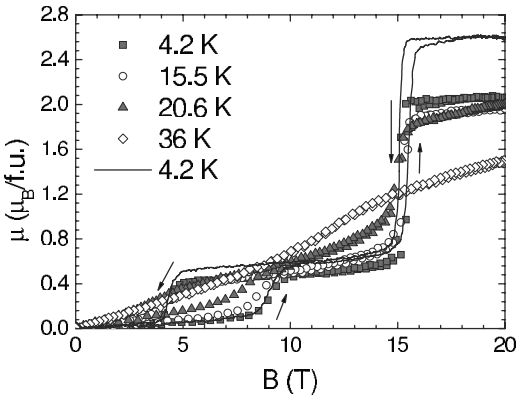

FIG. 10. High-field experiment on the mixed single-crystal sample (approximately 76.7% of α phase, and 23.3% of β phase). The field was applied along the c axis, which is common for both phases. To simplify the figure, we have plotted only representative curves. The solid line represents the recalculated data for 100% of the α phase.

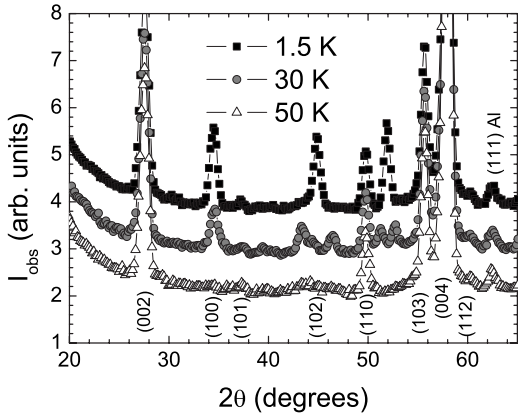

FIG. 11. Comparative neutron powder patterns for the α-$PrIr_2Si_2$. The peak at 62.9° is from the (111) reflection of the aluminum sample holder.

$PrCo_2Si_2$ [319(2) T] determined from Mössbauer experiments.[25,26]

The real part of the ac susceptibility (χ') measured for the α phase shows two distinct anomalies, which correspond to T_N and T_t, respectively (Fig. 8). The additional increase in χ' at temperatures below 10 K may be tentatively attributed to a tiny amount of an unknown ferromagnetic impurity phase. This idea is supported also by the jump of the imaginary part of the ac susceptibility (χ'') at temperatures around 5 K. Excepting the anomaly around 5 K on χ'', we observe an anomaly connected with T_t, but not with T_N.

The temperature dependence of the inverse dc susceptibility is shown in Fig. 9. The (001) (c axis) data differ considerably from those measured in the magnetic field applied within the basal plane. The conclusion is that, even in this crystallographic modification, there is only a negligible anisotropy within the basal plane and considerable anisotropy between the c axis and the basal plane. Contrary to β-$PrIr_2Si_2$, the c axis susceptibility for the α phase dominates the signal in the perpendicular directions, which implies the uniaxial magnetocrystalline anisotropy in α-$PrIr_2Si_2$ has the c axis as the easy-magnetization direction.

The susceptibility was fitted using the Curie-Weiss law (Fig. 9) and the fitted data are summarized in Table I. The fitted values of the effective moments again are somewhat higher than the effective moment calculated for a free Pr^{3+} ion. Analogous to β-$PrIr_2Si_2$, we attribute this discrepancy to the crystal-field effect which diverts the temperature dependence of the $1/\chi$ vs T dependence from the Curie-Weiss behavior.

For the magnetization study of α-$PrIr_2Si_2$, we performed a high-field experiment on the sample, which unfortunately consisted of a mixture of the α and β phase. As the c axis of the two phases in the sample were found to be parallel, the measurement of the c axis magnetization was feasible and the corresponding results are shown in Fig. 10. As the measured magnetization curves in the fields above 20 T saturate, we show data only for the magnetic fields up to 20 T to focus on the two observed steps. At 4.2 K, these steps occur at a magnetic field of around 8 T (with large hysteresis of several tesla) and at 15.5 T (with small hysteresis of approximately 0.5 T), respectively. Since there are no anomalies on the β-$PrIr_2Si_2$ magnetization curves measured for the magnetic field applied along the c axis (Fig. 4) and we have confirmed that the ordered magnetic moments in zero magnetic field are aligned along the c axis,[15] we suppose that the magnetization steps reflect a reorientation of the magnetic moments along the c axis in α-$PrIr_2Si_2$. This implies the presence of spin-flip metamagnetic transitions. The observed field hysteresis of the metamagnetic transitions and the smearing of the magnetization curves observed in the pulsed-field experiment in comparison with the measurements in static magnetic fields[15] is probably due to slow magnetic relaxations in comparison to the rapidly changing pulsed magnetic field.

After the high-field experiment, the measured sample was ground to a powder, and the x-ray analysis revealed that the sample contained 76.7% of α phase and 23.3% of the β phase. Since the c-axis signal of the β phase increases weakly and linearly with the magnetic field up to 40 T (see Fig. 4) we could calculate magnetic-moment data for the α phase using the formula $M_\alpha=(M_{meas}-0.233M_\beta)/0.767$, where M_α, M_{meas}, and M_β are the corresponding magnetic moments at the same magnetic field and temperature (calculated for the α phase and measured for the mixed phase and β-phase crystal). The recalculated data yield a magnetic moment of 2.6 μ_B/f.u. at $T=4.2$ K and $B=20$ T. The observed moment is, however, substantially smaller than the value expected for the free Pr^{3+} ion ($3.2\mu_B$/Pr). This discrepancy may be a result of not all of the Pr magnetic moments being oriented parallel in fields above the second metamagnetic transition (>15.5 T), or that a magnetic moment opposite to the magnetic field is induced on the Ir ions, or that the crystal field reduces the Pr magnetic moment.

To shed some more light on the $PrIr_2Si_2$ problem we performed neutron-diffraction experiments. The representative powder patterns collected at 1.5, 30, and 50 K are presented in Fig. 11. All peaks observed in the 1.5 K data can be indexed by integer hkl indices for the tetragonal unit cell. However, some of the peaks are not consistent with the extinction rules for the $I4/mmm$ space group. This suggests

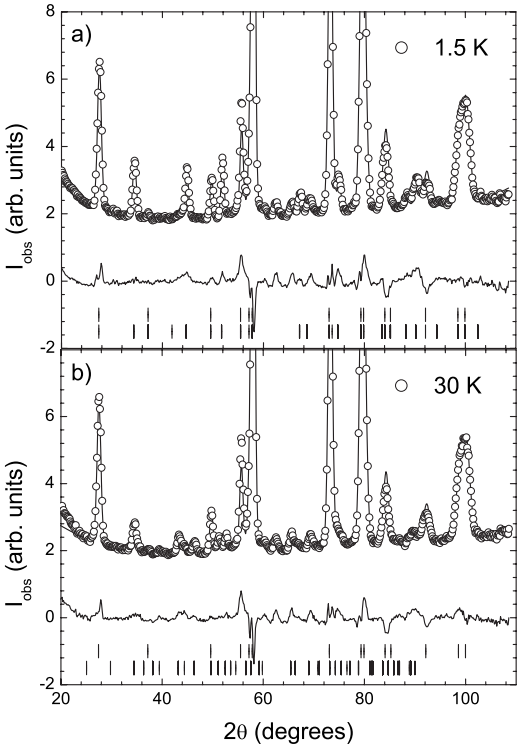

FIG. 12. Final Rietveld fit to the α-$PrIr_2Si_2$ data at (a) 1.5 K and (b) 30 K. The observed data are circles, the fit a solid line, and the difference curve is plotted below. The tick marks show the allowed reflections.

that the magnetic unit cell has the same dimensions as the nuclear unit cell but lower symmetry. Taking into account the magnetization measurements, all peaks can be indexed using a simple antiferromagnetic (AF) structure with the magnetic propagation vector $\boldsymbol{k}=(0\ 0\ 1)$ where the Pr magnetic moments are aligned along the c axis. Using this model, we successfully fitted the experimental data [Fig. 12(a)] and found that only the Pr ions possess stable magnetic moment. Our fit converged to the value of $3.2\mu_B$, which is equal to the theoretical magnetic moment of free Pr^{3+} ion.

At 30 K, splitting of the magnetic peaks to doublets [Fig. 12(b)] was observed. The assumption, therefore, is that the propagation vectors of the magnetic phases above and below T_t are not very different. Using this assumption and the positions of the magnetic reflections we estimated the magnetic propagation vector to be $\boldsymbol{k}=(0\ 0\ 0.9)$ as the starting point in the Rietveld fitting. As the first step we fitted only the c component of the magnetic propagation vector (k_c). The best fit was obtained for $k_c=0.836(3)$, close to 5/6, which was fixed. Subsequent refinement of the k_a and k_a did not improve the quality of the fit and it converged to $k_a \approx k_b \approx 0$. In case, we choose the $\boldsymbol{k}$ vector from the first Brillouin zone, we can describe our data also by the magnetic propagation vector (0 0 1/6). The decision to take (0 0 5/6) as the magnetic propagation vector for $T_t<T<T_N$ has been taken only with respect to its proximity to (0 0 1)—the magnetic propagation vector of the ground state. As the next step we tried to fit the size of the magnetic moment. As for the AF1 phase, our fit converged back to the value of $3.2\mu_B$.

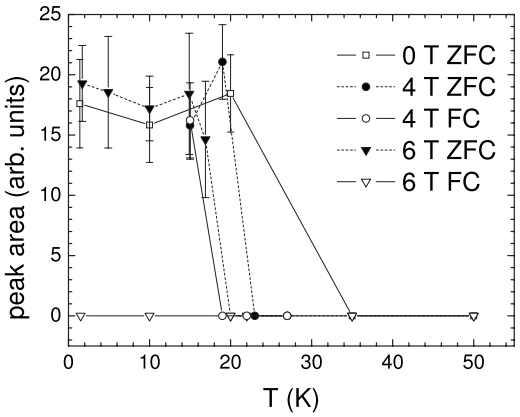

FIG. 13. The integrated intensity of $(-1\ -1\ 1)$ magnetic reflection with respect to temperature and to applied magnetic field.

Therefore, we conclude that α-$PrIr_2Si_2$ adopts in the temperature range $T_t<T<T_N$ a longitudinal sine-modulated magnetic structure with modulation along the c axis, $\boldsymbol{k}=(0\ 0\ 5/6)$, and with the stable magnetic moment on the Pr^{3+} ions of $3.2\mu_B$. Figure 12(b) shows the fit of our model with the experimental results. For both magnetic phases, we found a very satisfactory description of the magnetic phase using the magnetic moments localized only on the Pr^{+3} ions. Trials to add a small magnetic moment to the Ir atoms did not improve the fits. Therefore we can conclude that the iridium moment in this compound is lower than the resolution limit of the experiment ($0.2\mu_B$). As such, the scenarios where a magnetic moment associated with Ir is the reason for the discrepancies between the observed bulk magnetic data and the theoretical expectations can be discounted.

As a next step, we performed a single-crystal neutron-diffraction experiment to prove that the determined magnetic structure is correct. Since E6 has an area detector, to catch the whole reflection from this detector we have digitally masked it during the evaluation of the data with the mask 1.8° wide in 2θ, and 4° wide in ψ, and we had integrated through this area of the detector for each step in the ω scan. To obtain the full volume of the peak we have integrated such an obtained plot by the Gaussian function+linear background. Figure 13 represents our results of the magnetic $(-1\ -1\ 1)$ reflection. The maximum of this reflection occurs at 51.6(2)° in 2θ—in a good agreement with the neutron powder experiment [52.2(1)° from the powder pattern]. This reflection behaves completely as expected for the AF2 phase: Without applied magnetic field it has an invariable nonzero intensity in the temperature range 1.6–20 K and vanishes at higher temperatures. In a 6 T magnetic field in the zero-field-cooled (ZFC) run the intensity of this reflection is constant up to $T=15$ K within the experimental error, where the intensity begins to decrease and finally vanishes at 20 K. In the case of the FC run in a magnetic field of 6 T, the intensity of this reflection is zero for all measured temperatures (Fig. 13). This we consider as experimental proof for the field hysteresis region in which α-$PrIr_2Si_2$ can adopt either the low-magnetic field phase (AF2 phase) or the high-magnetic field phase. We confirmed this hysteresis region by ZFC and FC scans performed in the magnetic field of 4 T (see Fig. 13).

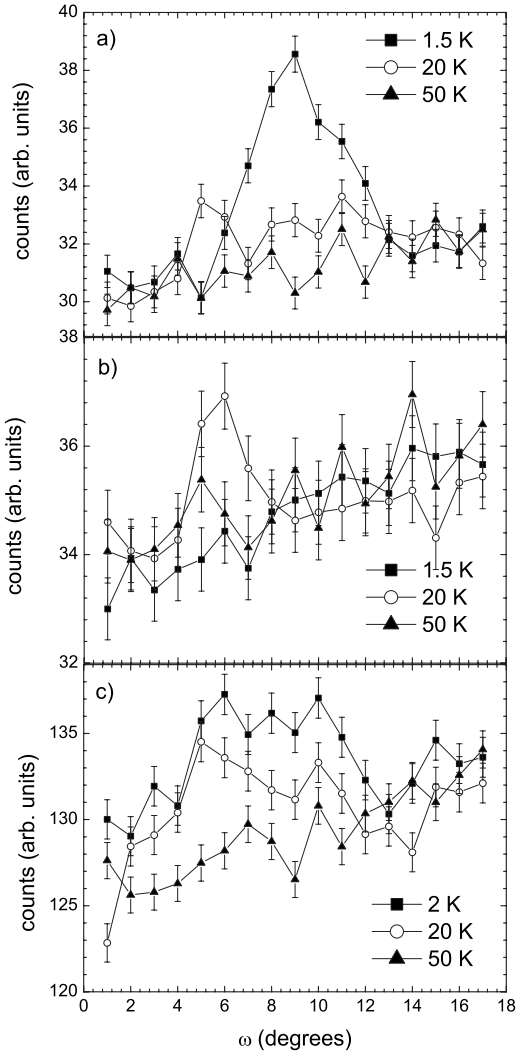

FIG. 14. The raw data scans from the single-crystal neutron-diffraction experiment on the α phase. The position ω=9°, 2θ=51.6° is the diffraction position for the (−1 −1 1) reflection. (a) The ZFC data obtained at B=6 T. The mask on the 2D detector was centered to 51.6° in 2θ. (b) The same scans as in (a) but the mask on the 2D detector was centered to 50.4°. (c) The FC data obtained at B=6 T. The mask on the 2D detector was centered to 51° in 2θ. To keep the figure simple, only representative scans are plotted.

Closer inspection of ZFC data measured in a magnetic field of 6 T [Figs. 14(a) and 14(b)] revealed an anomaly at 20 K located approximately −3° in ω from the (−1 −1 1) reflection with a maximum at 50.4(4)° in 2θ. This anomaly diminishes with increasing temperature and vanishes around 50 K. The corresponding FC data [Fig. 14(c)] exhibit the same type of anomaly, which was observed for temperatures 2 K, and 20 K, and centered at 50.6(4)° in 2θ. The ω and 2θ position of the anomaly is very close to the (−1 −1 5/6) reflection. The (−1 −1 5/6) reflection is one of the magnetic reflections of the AF1 phase as determined from the powder neutron-diffraction experiment performed in zero magnetic field. Nevertheless, we should bear in mind that now we measure the phase in a magnetic field above the first metamagnetic transition, which certainly cannot be antiferromagnetic because it is characterized by the magnetization of about 0.4–0.6 μ_B/f.u. (see Fig. 10) and therefore we deal with an uncompensated antiferromagnetic structure of a longer periodicity. A more detailed neutron-diffraction experiments with the α phase in magnetic fields is desired for determining the magnetic structure of the state above the first metamagnetic transition.

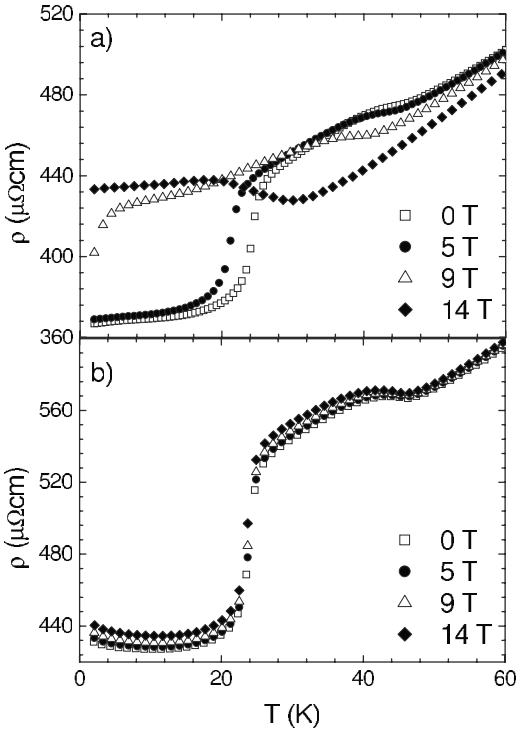

FIG. 15. The low-temperature detail of the resistivity of α-$PrIr_2Si_2$: (a) $i \| a$; $B \| c$; (b) $i \| c$; $B \| a$.

The electrical resistivity of α-$PrIr_2Si_2$ as a function of temperature and the magnetic field shows that, at temperatures higher than 60 K, this compound behaves as a normal metal. With decreasing temperature, the resistivity shows a slight increase below T_N (Fig. 15) and a considerable drop around T_t. Both the anomalies are shifted to lower temperature applying the magnetic field along the c axis, whereas the

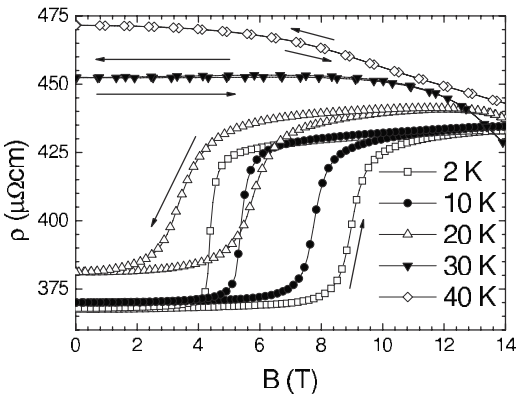

FIG. 16. The transverse magnetoresistivity of α-$PrIr_2Si_2$ in the experimental configuration $i \| a$; $B \| c$. The lines are guides for the eye.

temperature dependence of the resistivity remains almost intact in the *a*-axis magnetic field. This is consistent with the strong uniaxial magnetocrystalline anisotropy with the easy-magnetization direction along *c*. The magnetoresistance in the *c*-axis field is positive (negative) at temperatures lower (higher) than T_t. This result corresponds to the measured evolution of the magnetization and the expected long periodicity magnetic structure (uncompensated antiferromagnetism) in the *c*-axis magnetic field sufficient to induce in the first metamagnetic state.

The resistivity variations at the magnetic phase transitions (Figs. 15 and 16) are closely connected with the corresponding changes of the magnetic periodicity with respect to the crystallographic periodicity. In the case of the AF1 phase the magnetic unit cell is (considerably) larger than the crystallographic unit cell. As a result when the border from the AF2 phase to the AF1 phase at T_t is crossed, the new energy gaps appear at the Brillouin-zone boundaries and the resistivity increases. When the boundary between the AF2 phase and the high-field induced state is crossed, the symmetry again changes.

One can also see that the anomalies on the magnetoresistance curves in Fig. 16 well reflect the metamagnetic transition observed on the magnetization curves in Fig. 10 including the large field hysteresis. Unfortunately the maximum magnetic field of the PPMS apparatus (14 T) is about 1 T lower than the critical field (B_{c2}) for the second metamagnetic transition seen on the magnetization curves in Fig. 16. Since the second metamagnetic state is most probably characterized by a ferromagneticlike arrangement of Pr magnetic moments, the resistivity above the second metamagnetic transition ($B > B_{c2}$) should be dramatically reduced with respect to the first metamagnetic state because the ferromagneticlike structure is much more coherent with respect to the long period uncompensated AF (UAF) phase (existing for $B_{c1} < B < B_{c2}$). The onset of this decrease can be already observed in the 20 K data in Fig. 16.

IV. DISCUSSION

The main issues of this paper are the striking differences in physics of $PrIr_2Si_2$ related to the two crystallographic modifications. The formation of one of the two modifications is closely dependent on the thermal history. The α phase is stable at room temperature and lower temperatures and can be obtained by sufficiently slow cooling from high temperatures (>1000 K). The β phase is stable only at high temperatures, nevertheless it can be also obtained at room temperature (as a metastable phase) by rapid quenching of the sample.

This has been found not only for $PrIr_2Si_2$ but also for the series $REIr_2Si_2$ compounds (*RE*=La through Nd). Both the structures are tetragonal; each is characterized by a specific stacking of the *RE*, Ir, and Si atomic layers along the *c* axis. α-$REIr_2Si_2$ adopts a centrosymmetric structure (space group $I4/mmm$) due to the symmetric stacking of *RE*–Si–Ir–Si–*RE*–Si–Ir–Si–*RE* around the inversion center, which contains a *RE* ion. The atomic layer stacking *RE*–Ir–Si–Ir–*RE*–Si–Ir–Si–*RE* makes the β phase non-

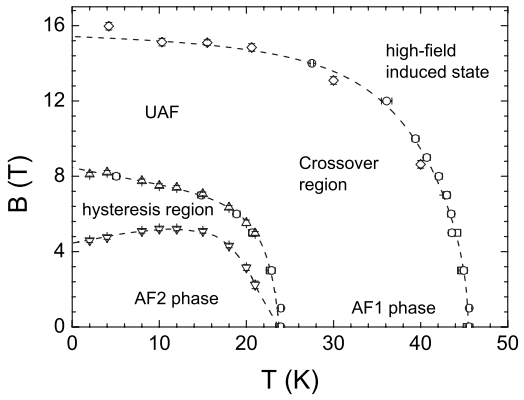

FIG. 17. The phase diagram of the α phase for the magnetic field applied along the *c* axis constructed using the specific-heat data (squares), $M(T)$ data (circles), static field $M(B)$ data (both types of triangles), and pulsed magnetic field data (diamonds). The lines are only guides for the eye.

centrosymmetric; the crystallographic unit cell is primitive (space group $P4/nmm$).

It is well known that when a non-Kramers ion such as Pr^{3+} is located in a low symmetry crystal field, each of its multiplet should be split into $2J+1$ singlets. If the gap between the ground state and the first excited state is sufficiently large, a nonmagnetic ground state is usually observed. The Pr^{3+} ion in the α-$PrIr_2Si_2$ appears in a center of symmetry of the tetragonal crystal field owing to the Pr–Si–Ir–Si–**Pr**–Si–Ir–Si–Pr stacking. In the β phase, the crystal field that the Pr site feels is highly nonsymmetric due to the Pr–Ir–Si–Ir–**Pr**–Si–Ir–Si–Pr sequence of atomic layers.

In both α-$PrIr_2Si_2$ and β-$PrIr_2Si_2$ we have found strong crystal-field attributes in our results: the Schottky contribution to the specific heat (Fig. 2), the strong magnetocrystalline anisotropy well documented by the low-temperature magnetization curves (Figs. 3, 9, and 10) and a feature in the temperature dependence of the electrical resistivity of β-$PrIr_2Si_2$ (Fig. 5). In the β phase, which stays paramagnetic to the lowest temperatures of our measurements, the strong magnetocrystalline anisotropy yields the dominant magnetization signals perpendicular to the *c* axis; i.e., one can speak about easy basal plane anisotropy. In the α phase, the symmetric tetragonal crystal field causes uniaxial anisotropy with the *c* axis as the easy-magnetization direction.

In order to obtain a quantitative estimate of the crystal-field (CF) interaction in the two $PrIr_2Si_2$ phases, first-principles calculations based on density-functional theory (DFT) using the method described in the work of Diviš *et al.*[27] were performed. Using this method the electronic structure and the corresponding distribution of the ground-state charge density are obtained using the full-potential linearized augmented plane wave plus local orbitals method. The crystal-field parameters originate from the aspherical part of the total single-particle DFT potential in the crystal. To eliminate the self-interaction, the self-consistent procedure is first performed with the 4*f* electrons as core (open-core approximation). Using this method the correct sign of the crystal-field anisotropy in both $PrIr_2Si_2$ phases, which is gov-

erned by the sign of parameter B_{20} in the microscopic CF Hamiltonian, has been obtained. We did not fit the crystal-field parameters since the CF Hamiltonian contains five terms in the case of the tetragonal symmetry. Thus the possibility of finding multiple solutions is very high.

The strong uniaxial anisotropy in α-$PrIr_2Si_2$ means that the magnetic structure is stable for the field applied along the a axis up to at least 14 T (derived from the resistivity measurements) but applying comparable magnetic fields along the c axis causes the collapse of the ground-state magnetic structure and brings the sample to the field-induced ferromagneticlike state in fields higher than 15.5 T (at 4.2 K) as observed by the high-field magnetization measurements. The observed magnetization in the high-field forced state ($\mu \approx 2.6\ \mu_B$/f.u.) is substantially smaller than the value determined by the neutron-diffraction experiment in zero magnetic field ($3.2\mu_B$/Pr). The latter is equal to the theoretical value of the ordered magnetic moment of the free Pr^{3+} ion. Considering these results two scenarios are available to elucidate this discrepancy: (a) an Ir magnetic moment of $\sim 0.4\mu_B$ oriented opposite to the Pr magnetic moment is induced at the 15.5 T transition, where the Pr magnetic moments align "ferromagnetically" (b) not all the Pr magnetic moments above 15.5 T are aligned parallel. A neutron single-crystal experiment in a magnetic field above 15.5 T (not yet readily available on neutron beamlines) applied along the c axis may help resolving this question.

The results of our bulk and neutron-diffraction experiments allow the extension of the B-T (for $B \| c$) magnetic phase diagram presented earlier[15] to that presented in Fig. 17. In zero field we distinguish two different antiferromagnetic phases. The ground-state AF2 phase is stable for $T < T_t$ and $B < B_{C1}$. When the magnetic field is increased, a metamagnetic phase transition to the first (second) metamagnetic state is observed at B_{C1} (B_{C2}). The first metamagnetic phase is characterized by a small nonzero bulk magnetic moment (~ 0.5–$0.6\ \mu_B$/f.u.). The neutron single-crystal diffraction experiment on α-$PrIr_2Si_2$ in magnetic fields points to a periodicity of this phase around $6c$. In fields $> B_{C1}$, a high-field metamagnetic state is realized, probably "ferromagneticlike" with all Pr moments parallel. A reliable neutron-diffraction experiment in fields higher than B_{C2} is, however, crucial in order to confirm (or correct) this idea.

The AF1 phase is stable in zero magnetic field at temperatures $T_t < T < T_N$ in zero magnetic field and the neutron-diffraction data point to the periodicity around $6c$. Further detailed neutron scattering or μSR studies, however, should be performed to resolve whether this phase is commensurate or incommensurate. The magnetization curves measured at temperatures $T_t < T < T_N$ do not show any distinct metamagnetic transition but are characterized by a high slope yielding a comparable magnetic moment to the first metamagnetic phase (when $T < T_t$ and $B < B_{C1}$) in fields around 6 T and increase with magnetic field. The smeared magnetization (Fig. 10 in this paper and Fig. 10 in Ref. 15) and magnetoresistance (Fig. 16) can be understood as documenting the continuous crossover from the zero-field AF1 phase to the second metamagnetic state (possibly across the UAF state). An extended neutron single-crystal diffraction study as a function of magnetic field and temperature should be performed to elucidate this transformation in detail on the microscopic level.

At temperatures below T_t there is considerable region of hysteresis in which the α phase can adopt both the AF1 and UAF phase depending on the thermomagnetic history of the sample. The maximum field applied along the c axis, which will destroy the AF1 phase, and forces the field-induced alignment of the Pr magnetic moments in is 15.5 T at 4.2 K. The stability of the AF2 phase in a magnetic field lower than B_{C1} and the hysteresis region has been unambiguously confirmed by the single-crystal neutron-diffraction experiment (Fig. 13).

Our magnetic phase diagram for α-$PrIr_2Si_2$ has features similar to the magnetic phase diagrams of HoAlGa (Ref. 28) and $PrCo_2Si_2$.[29,30] In comparison with HoAlGa we have found the similarities in the transition from an incommensurate to a commensurate magnetic phase but instead of phase III we have found the hysteresis region in α-$PrIr_2Si_2$. This difference might be caused by the different crystal structure of the two compounds and, consequently, the different crystal field acting on the rare-earth ions.

If we compare $PrCo_2Si_2$ and α-$PrIr_2Si_2$, we find that both the compounds crystallize in the same crystallographic structure and, hence, one should expect a similar crystal field acting on the Pr^{3+} ions. The magnetic ground state is antiferromagnetic in both compounds with the propagation vector $\boldsymbol{k}=(0\ 0\ 1)$. In case of $PrCo_2Si_2$, there exist two more magnetic phases (in zero field) (Ref. 29) compared to only one additional magnetic phase for α-$PrIr_2Si_2$. Also the propagation vector for the AF1 phase of α-$PrIr_2Si_2$ is in between (0 0 0.926) and (0 0 0.777), previously reported for $PrCo_2Si_2$.[29] The ordering temperatures to the magnetic ground state and the temperature of the phase transition from paramagnetic to the magnetically ordered state is substantially higher for α-$PrIr_2Si_2$ than for $PrCo_2Si_2$ [$T_N=45.5$ K and $T_t=23.7$ K for α-$PrIr_2Si_2$ and $T_N=30$ K, $T_2=17$ K, and $T_1=9$ K for $PrCo_2Si_2$ (Ref. 29)], which points to somewhat different interplay between the exchange and crystal-field interactions.

An important question remains why $PrIr_2Si_2$ exhibits such contrasting magnetic properties in the two phases. While both involved crystal structures are tetragonal, the Pr ions bearing magnetic moments appear in dramatically different coordination of ligands. For the $ThCr_2Si_2$ type (space group $I4/mmm$) the Pr ion feels mainly the highly symmetric crystal field due to eight Si nearest neighbors, whereas in the $CaBe_2Ge_2$-type structure (space group $P4/nmm$) the Pr ion appears within a lower symmetry environment with four Ir and four Si nearest neighbors. The lower symmetry of the crystal field probably leads to the singlet ground state of the Pr^{3+} ion, which implies lack of low-temperature magnetic ordering. The higher symmetry of the Pr neighborhood also promotes stronger exchange interactions, which yield better conditions for magnetic ordering.

V. CONCLUSIONS

We have studied the magnetism of α-$PrIr_2Si_2$ and β-$PrIr_2Si_2$. We have confirmed that the β phase does not order magnetically down to 2 K, nevertheless it shows

strongly anisotropic magnetization due to a strong crystal-field effect. As concerns the magnetism in the α-$PrIr_2Si_2$, we have confirmed that this crystallographic modification undergoes two magnetic phase transitions, from paramagnetic to the sine-modulated magnetic structure with modulation along the c axis at T_N=45.5(1) K and with a magnetic propagation vector of approximately $\boldsymbol{k}$=(0 0 5/6). The subsequent transition occurs at T_t=23.7 K to the ground-state simple antiferromagnetic structure. In both magnetic phases the stable magnetic moment was observed by neutron diffraction to be only on the praseodymium ions ($\mu_{Pr}=3.2\mu_B$). This value compares well with the theoretical ordered magnetic moment of the free Pr^{3+} ion, which suggests that the Pr magnetic moment is localized and the praseodymium is trivalent in this compound. The AF phases can be destroyed by sufficiently high magnetic fields, however, the "saturated" magnetic moment observed by high-field magnetization measurements for $B>B_{C2}$ is considerably lower. This observed discrepancy leaves an open question about the magnetic state in high magnetic fields above the upper metamagnetic transition, which may be resolved by future neutron single-crystal diffraction experiments when magnetic fields well above 15.5 T will be available at neutron beamlines.

An important issue discriminating physics of the two crystallographic modifications of $PrIr_2Si_2$ is the symmetry of the magnetocrystalline anisotropy, which is strong in both cases irrespective to the ground state. The α phase exhibits uniaxial anisotropy with the c axis as the easy-magnetization direction whereas in the β phase the signal in directions within the basal plane dominates the c-axis magnetization. Results of our *ab initio* crystal-field calculations are in agreement with the experimental findings.

ACKNOWLEDGMENTS

This work is a part of the research plan MSM Grant No. 0021620834 that is financed by the Ministry of Education of the Czech Republic. The work of M.D. and V.S. was also supported by the Czech Grant Agency (Project No. 202/09/1027). Neutron scattering experiments were supported by the European Commission under the Sixth FP through the Key Action: Strengthening the European Research Infrastructures, Contract No. RII3-CT-2003-505925 (NMI 3). High-magnetic field experiments were performed within the EuroMagNET under the EU under Contract No. RII3-CT-2004-506239. The authors thank P. Henry for careful reading and correcting the manuscript.

*Present address: Helmholtz-Centre Berlin for Materials and Energy, Hahn-Meitner-Platz 1, 14109 Berlin, Germany; matus.mihalik@helmholtz-berlin.de

[1] H. F. Braun, N. Engel, and E. Parthé, Phys. Rev. B **28**, 1389 (1983).
[2] R. Hoffmann and C. Zheng, J. Phys. Chem. **89**, 4175 (1985).
[3] E. H. El Ghadraoui, J. Y. Pivan, R. Guérin, O. Pena, J. Padiou, and M. Sergent, Mater. Res. Bull. **23**, 1345 (1988).
[4] W. Jeitschko, W. K. Hofmann, and L. J. Terbuchte, J. Less-Common Met. **137**, 133 (1988).
[5] T. Endstra, G. J. Nieuwenhuys, A. A. Menovsky, and J. A. Mydosh, J. Appl. Phys. **69**, 4816 (1991).
[6] D. Niepmann and R. Pöttgen, Intermetallics **9**, 313 (2001).
[7] Z. Hossain, C. Geibel, F. Weickert, T. Radu, Y. Tokiwa, H. Jeevan, P. Gegenwart, and F. Steglich, Phys. Rev. B **72**, 094411 (2005).
[8] R. Welter, K. Halich, and B. Malaman, J. Alloys Compd. **353**, 48 (2003).
[9] W. X. Zhong, B. Lloret, W. L. Ng, B. Chevalier, J. Etourneau, and P. Hagenmuller, Rev. Chim. Miner. **22**, 711 (1985).
[10] M. Mihalik, Z. Matěj, and V. Sechovský, Intermetallics **17**, 927 (2009).
[11] M. Mihalik, M. Diviš, and V. Sechovský, Physica B **404**, 3191 (2009).
[12] T. Wiener, I. Fisher, and P. Canfield, J. Alloys Compd. **303-304**, 289 (2000).
[13] A. Garnier, D. Gignoux, D. Schmitt, and T. Shigeoka, Physica B **212**, 343 (1995).
[14] M. Mihalik, J. Vejpravová, J. Rusz, M. Diviš, P. Svoboda, V. Sechovský, and M. Mihalik, Phys. Rev. B **70**, 134405 (2004).
[15] M. Mihalik, M. Diviš, and V. Sechovský, J. Magn. Magn. Mater. **322**, 1153 (2010).
[16] www.helmholtz-berlin.de/user/neutrons/instrumentation/neutron-instruments/e6_en.html
[17] www-llb.cea.fr/fullweb/fp2k/fp2k_os.htm4
[18] W. R. Busing and H. A. Levy, Acta Crystallogr. **22**, 457 (1967).
[19] www.ifw-dresden.de/institutes/imw/sections/22/laboratory-for-pulsed-high-magnetic-fields/setup-1/setup
[20] C. Kittel, *Úvod do fyziky pevných látek* (Academia, Praha, 1985).
[21] M. Rotter, M. Doerr, M. Loewenhaupt, U. Witte, P. Svoboda, J. Vejpravová, H. Sassik, C. Ritter, D. Eckert, A. Handstein, and D. Hinz, Phys. Rev. B **64**, 134405 (2001).
[22] N. W. Ashkroft and N. D. Mermin, *Solid State Physics* (Saunders College, Philadelphia, 1976).
[23] M. Mihalik, H. Kitazawa, M. Diviš, and V. Sechovský, J. Alloys Compd. **460**, 26 (2008).
[24] J. E. Gordon, C. W. Dempsey, and T. Soller, Phys. Rev. **124**, 724 (1961).
[25] B. D. Dunlap and G. M. Kalvius, in *Theory of Isomer Shifts*, edited by G. K. Shenoy and F. E. Wagner (North-Holland, Amsterdam, 1978).
[26] A. A. Moolenaar, Ph.D. thesis, TU Delft, 1994.
[27] M. Diviš, J. Rusz, H. Michor, G. Hilscher, P. Blaha, and K. Schwarz, J. Alloys Compd. **403**, 29 (2005).
[28] A. R. Ball, D. Gignoux, D. Schmitt, and F. Y. Zhang, Phys. Rev. B **47**, 11887 (1993).
[29] M. Motokawa, H. Nojiri, and Y. Endoh, Physica B **177**, 279 (1992).
[30] T. Shigeoka, N. Iwata, H. Fujii, T. Okomato, and Y. Hashimito, J. Magn. Magn. Mater. **70**, 239 (1987).